ELSEVIER

Tumor model-specific proviral insertional mutagenesis of the *Fos/Jdp2/Batf* locus

M.H. Rasmussen[a], A.B. Sørensen[a], D.W. Morris[b,1], J.C. Dutra[b,2], E.K. Engelhard[b,3], C.L. Wang[c], J. Schmidt[d], F.S. Pedersen[a,*]

[a]*Department of Molecular Biology, University of Aarhus, C. F. Mollers Allé, Building 130, DK-8000 Aarhus C, Denmark*
[b]*Sagres Discovery, Davis, CA 95617, USA*
[c]*Department of Microbiology and Immunology, University of California-San Francisco, San Francisco, CA 94143, USA*
[d]*Department of Comparative Medicine, GSF-National Research Center for Environment and Health, D-85764 Neuherberg, Germany*

Abstract

Retroviral activation of the AP-1/ATF super family member *Jdp2* was recently reported to be a common event in M-MLV-induced T cell lymphoma in p27-null C57x129 mice as compared to wild type-inoculated mice but has not been found important in other models. On the basis of retroviral tag retrieval from 1190 individual Akv- and SL3-3-induced lymphomas, we here report that insertional mutagenesis into the 250-kb *Fos/Jdp2/Batf* locus is associated with SL3-3 MLV-induced T but not Akv-induced B cell lymphomas of NMRI and SWR mice. Integration pattern and clonality analyses suggest that Jdp2 participates in SL3-3-induced tumorigenesis distinctly as compared to the M-MLV setting. Northern blot analysis showed *Jdp2* to be alternatively spliced in various normal tissues as well as MLV-induced lymphomas. Interestingly, in some tumors, proviral insertion seems to activate different mRNA sub-species. Whereas elevated mRNA levels of the *Fos* gene could not be correlated with provirus presence, in one case, Northern blot analysis as well as quantitative real-time PCR indicated proviral activation of the AP-1 super family member *Batf*, a gene not previously reported to be a target of insertional mutagenesis. A novel integration cluster between *Jdp2* and *Batf* apparently did not influence the expression level of either gene, underscoring the importance of addressing expression effects to identify target genes of insertion. Altogether, such distinct insertion patterns point to different mechanism of activation of specific proto-oncogenes and are consequently of importance for the understanding of proviral activation mechanisms as well as the specific role of individual oncogenes in tumor development.
© 2005 Elsevier Inc. All rights reserved.

Keywords: Mutagenesis; Tumor; Oncogene; Provirus; SL3-3; *Jdp2*; *Batf*

Introduction

The deregulation of critical host genes by insertional mutagenesis is believed to be an important step in induction of hematopoietic cancers in mice infected with the murine leukemia viruses (MLV) (Rosenberg and Jolicoeur, 1997). Multiple events of cooperating retroviral insertions contribute to cellular clonal expansion and eventually the development of a full-blown tumor. Identification of insertion site positions (retroviral 'tags' (Sørensen et al., 1996)) has proven to be a potent in vivo genetic screen for cancer-related genes; and this strategy is currently yielding an explosion of data with the assembly of the mouse genome draft, which enables high-throughput insertion site positioning on a chromosomal scale. This is amply demonstrated with the collective description by recent large-scale tagging efforts of several hundreds putative onco-loci among thousands of integration sites from various virus/host models

---

(Erkeland et al., 2004; Hansen et al., 2000; Hwang et al., 2002; Johnson et al., 2005; Joosten et al., 2002; Kim et al., 2003; Li et al., 1999; Lund et al., 2002; Mikkers et al., 2002; Sørensen et al., 1996; Suzuki et al., 2002), many of which are accessible online in the Retroviral Tagged Cancer Gene Database (RTCGD) (http://www.rtcgd.ncifcrf.gov/) (Akagi et al., 2004). An interesting pattern that emerges from the growing catalog of tags is that whereas some integration sites appear common to a broader set of models, other integration sites are distinct to single systems. Since the integration distribution of end-stage tumors reflects the selection process of tumorigenesis, comparing model-specific integration patterns may be assumed to offer insights into distinct participations of individual oncogenes during tumor development, but equally important, also reveals insights into the mechanisms behind different pathogenic responses in individual virus/host systems. Hence, defining model-specific integration patterns by comparative tag analysis will offer essential information for future classification of lymphatic malignancies.

Jdp2 encodes a small protein belonging to the AP-1/ATF super family of transcriptional regulators. It was originally identified as a repressive dimerization partner to Jun (Aronheim et al., 1997) but also represses Atf2-mediated transcription (Jin et al., 2001), and may associate with the CCAAT/enhancer-binding protein γ (Broder et al., 1998), histone deacetylase 3 complex (Jin et al., 2002) as well as with the progesterone receptor (Wardell et al., 2002). *Jdp2* is ubiquitously expressed and appears to be subject to complex, tissue-specific splicing regulation (Jin et al., 2001). The role of Jdp2 in tumor development is controversial. On one hand, Jdp2 induces differentiation of osteoclasts (Kawaida et al., 2003) and myoblasts (Ostrovsky et al., 2002) and inhibits transformation of NIH fibroblast cells and tumor development in SCID mice (Heinrich et al., 2004). On the other hand, its overexpression leads to partial transformation of chick embryo fibroblasts (Blazek et al., 2003) and repression of tumor-suppressor p53-induced apoptosis in UV-exposed fibroblasts (Piu et al., 2001). In support of a tumorigenic role, Hwang et al. recently described an enhanced frequency of proviral insertional activation of *Jdp2* in lymphomas from Moloney MLV (M-MLV) inoculated p27-null C57/B6J × 129/Sv mice as compared to M-MLV inoculated wild type mice (Hwang et al., 2002).

From a comparative tag analysis study involving Akv and SL3-3 MLV, we report insertion within and around *Jdp2* to be a frequent event of SL3-3 induced lymphomagenesis with notable differences to the M-MLV setting regarding clonality and clustering of integration sites and describe proviral induction of alternative *Jdp2* RNA sub-species. We also report proviral activation of the *Jdp2* neighboring gene *Batf*. *Fos*, the last gene of the locus was not influenced by the insertions.

Results

Proviral insertion into the Fos/Jdp2/Batf locus

Our attention to *Jdp2* was initially drawn by the finding of two closely spaced SL3-3-derived proviruses in, what was at that time, an unknown chromosomal region ((Sørensen et al., 1996) and H. Moving, unpublished) (in mice s3 and s10 in Fig. 1). Since then, we have isolated proviral integration sites from a range of murine lymphomas induced by the T cell lymphomagenic SL3-3 MLV, the B cell lymphomagenic Akv MLV and derivatives of the two. In total, roughly 5000 tags have been isolated from 1190 animals inoculated (see Materials and methods). With this screen, 22 integrations have been found in a 250-kb region on mouse chromosome 12 encompassing *Jdp2* as well as two other AP-1/ATF super family members *Fos* and *Batf* (Fig. 1). Table 1 shows the number of animals subjected to retroviral tagging and the number of *Fos/Jdp2/Batf* locus integrations found within each model as defined by virus (irrespectively of sub-type) and mouse strain. The tumors were for the most part isolated from diseased animals injected with SL3-3 or an SL3-3 derivative (Table 2). The SL3-3 derivates harbor consecutive triple-base mutations in the Runx site I, site II or both (Hallberg et al., 1991), triple-base mutation in the upstream conserved region (UCR) (Ma et al., 2003) and an SL3-3 enhancer variant, SL3-3(2Δ18-3 1/2) (hereafter referred to as SL3-3 Turbo), with increased pathogenicity as compared to wild type SL3-3 (Ethelberg et al., 1997c; Nielsen et al., 2005). Three tumors originated from panels with co-injections of Akv1-99 (a single enhancer repeat variant of Akv (Lovmand et al., 1998)) derivatives with mutations in the Runx or the E-box E_{GRE} motifs and SL3-3 wild type (unpublished results). In all
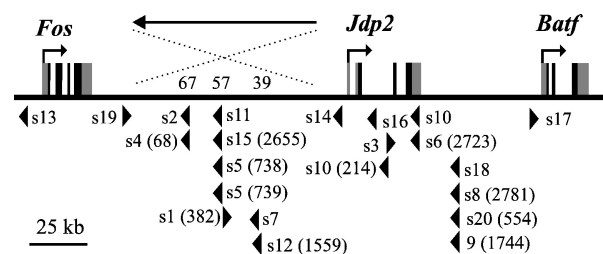

Fig. 1. The *Fos/Jdp2/Batf* locus. Position and transcriptional orientation of individual proviruses are indicated by triangles according to our corrected sequence of clone fragments (see text). Each provirus is identified by the name of the mouse from which it was isolated (two proviruses in the locus were identified in mice s5 and s10). The distance (in base pairs) to the preceding proviruses within clusters is shown in parenthesis. Note that one of the proviruses identified in s10 lies within the 3′ UTR of *Jdp2* whereas that in s6 is positioned outside. Also shown is the distance (in kb) from *Jdp2* to the first provirus of the *Fos/Jdp2* intergenic clusters, and the extent of the apparently erroneous inverted UCSC clone fragments (October 2003 assembly) are indicated with an arrow opposite to the transcriptional orientation of the locus. In the May 2004 assembly, this inversion apparently has been corrected. The gene structure of the three RefSeq annotated genes of the locus (transcription from left to right) is indicated with coding sequence in black and UTRs in grey.

Table 1
Distribution of *Fos/Jdp2/Batf* locus integrations among virus/host models

Model[a]	No. of mice tagged (No. of mice with *Fos/Jdp2/Batf* integrations)	Total
Akv/NMRI-i	524 (2)	
Akv/SWR	37 (0)	561 (2)
SL3-3/NMRI-r	58 (5)	
SL3-3/NMRI-i	327 (6)	
SL3-3/SWR	98 (4)	470 (15)
Akv + SL3-3/NMRI-i	159 (3)[b]	159 (3)
		1190 (20)

  [a] Mice in this study were SWR, and inbred and random-bred NMRI mice (NMRI-i and NMRI-r, respectively).
  [b] The three *Fos/Jdp2/Batf* locus integrations from Akv and SL3-3 co-injected panels (see Table 2 and text) were SL3-3 derived.

three cases, directed PCR and sequencing determined that the specific provirus in the *Fos/Jdp2/Batf* locus was derived from SL3-3 (not shown). One panel came from co-injection of Akv wt and an Akv1-99 variant with mutations in Runx and the glucocorticoid receptor (GR) binding motifs. Finally, one panel of tumors was induced by an Akv with altered primer binding (PBS) site (Pro to Lys) (unpublished results) and one induced by an SL3-3 with the non-LTR UTR replaced by that of Akv (Lund et al., 1999). The panels differ with regard to mouse strain; both random-bred and inbred NMRI as well as SWR are included (Table 1). Both strains lack endogenous ecotropic proviruses, and are susceptible to SL3-3 and Akv induced

lymphomagenesis. There is an overwhelming bias towards SL3-3 integration into the *Fos/Jdp2/Batf* locus (Table 1) with only two Akv derived proviruses at the extremities of the locus (Fig. 1). Any correlation to a specific model is less clear, albeit we notice a skew toward the SL3-3 /NMRI-r and SL3-3/SWR models, with five and four integrations identified from 58 and 98 mice, respectively. There was no correlation between integration in the locus and latency of the individual mouse as compared to mean latency of the particular panel (Table 2).

When aligned against public draft sequences (http://www.ensembl.org and http://www.genome.ucsc.edu), the majority of the *Fos-Jdp2* integrations were in positive orientation with respect to *Fos* and *Jdp2*. The same integrations turned out to influence *Jdp2* expression but not *Fos* (see below), and given the predominantly observed head–head virus–host gene orientation among other common integration sites, we investigated the possibility of erroneous assembly of the current draft sequence. Indeed, Southern blot hybridizations against the extremities of clone fragments on digested BAC DNA covering the region (not shown) suggested a 90-kb inversion (base position 81.491.892 to 81.602.893) involving fragments CA-AA01071983.1, CAAA01071982.1 and AC115037.3 (UCSC October 2003 assembly) as shown in Fig. 1. We note that for genomic regions targeted by provirus integration, the proviral orientational bias could be instrumental in general to identify possible erroneous assemblies of the draft genome.

Table 2
Tumor panels with mice harboring integration in the *Fos/Jdp2/Batf* locus

Mouse	Virus[a]	Mouse strain[b]	Lymphoma incidence[c]	Mean latency (days) (SD)	Tumor phenotype	No. of mice tagged	Latency of *Fos/Jdp2/Bat* mouse
s1	SL3-3 Runx II	NMRI-r	109/111	101 (40)	T	27	102
s2	SL3-3 Runx II	NMRI-r	109/111	101 (40)	T	27	99
s4	SL3-3 Runx I	NMRI-r	28/46	266 (144)	T	11	146
s5	SL3-3 Runx I	NMRI-r	28/46	266 (144)	T	11	196
s10	SL3-3 Runx dm	NMRI-i	12/12	248 (38)	mixed	7	236
s6	SL3-3 UCR328s	SWR	10/11	93 (22)	T	10	121
s7	SL3-3 UCR330s	SWR	20/20	80 (19)	T	18	62
s8	SL3-3 UCR332s	SWR	23/27	82 (16)	T	16	96
s9	SL3-3 wt	SWR	9/9	107 (29)	T	7	76
s3	SL3-3 wt	NMRI-r	49/49	92 (33)	T	20	124
s12	SL3-3 wt	NMRI-i	20/20	60 (5)	T	18	68
s20	SL3-3 wt	NMRI-i	40/40	56 (8)	T	40	52
s11	SL3-3 wt/Akv UTR	NMRI-i	20/20	56 (7)	T	17	55
s13	Akv PBS$_{Lys}$	NMRI-i	20/20	206 (30)	n.d.	20	234
s14	Akv1-99 Runx + SL3-3 wt	NMRI-i	41/43	126 (40)	n.d.	40	88
s17	Akv1-99 Runx/GR + Akv wt	NMRI-i	53/53	188 (31)	n.d.	53	232
s15	Akv1-99 Egre + SL3-3 wt	NMRI-i	48/50	148 (47)	n.d.	38	94
s16	Akv1-99 Egre + SL3-3 wt	NMRI-i	48/50	148 (47)	n.d.	38	99
s18	SL3-3 Turbo	NMRI-i	115/115	49 (6)	T	115	47
s19	SL3-3 Turbo	NMRI-i	115/115	49 (6)	T	115	48

  [a] The viruses mentioned here originated from published (Ethelberg et al., 1997b, 1997c; Hallberg et al., 1991; Lund et al., 1999; Ma et al., 2003; Nielsen et al., 2005; Sørensen et al., 1996, 2004) as well as unpublished pathogenicity studies (see text).
  [b] Mice in this study were SWR and inbred and random-bred NMRI mice (NMRI-i and NMRI-r, respectively).
  [c] No. of mice from the particular injection round with enlarged lymphoblastic organs observed upon necropsy/no. of mice injected.

As seen for other common integration loci, integrations were clustered into discrete regions throughout the locus, the cluster 57 kb upstream of *Jdp2* being the most populated (Fig. 1). This contrasts the integration pattern observed in M-MLV mediated activation of *Jdp2* in which most proviruses integrated into intron 2 or exon 4 and in the same transcriptional orientation as *Jdp2* (Hwang et al., 2002). Of the intragenic SL3-3 proviruses, only one (in s3) could allow production of chimeric transcripts. Finally, we found an integration cluster between *Jdp2* and *Batf* unique to the SL3-3 model. The distinct integration pattern suggested different participation of the viruses in the two models, which encouraged us to further characterize the individual tumors with *Fos/Jdp2/Batf* insertion.

T cell lymphoma characterization

Animals diseased from MLV injections generally showed gross enlargement of thymus, spleen and peripheral lymph nodes. To determine the phenotype of the lymphomas with integration in *Fos/Jdp2/Batf*, Southern blot hybridization with probes recognizing clonal rearrangements of the Ig κ chain locus and the TCR β chain locus was done as described previously (Ethelberg et al., 1997a). We isolated DNA from tumor tissues of mice harboring proviral insertion in the *Fos/Jdp2/Batf* locus as well as from animals from the same panels but in which integrations in this locus were not found (control animals). Table 3 summarizes the results. Tumors from panels with SL3-3-inoculated animals

Table 3
Summary of characterization of tumors harboring *Fos/Jdp2/Batf* provirus integration

Mouse	Tissue[a]	Provirus status[b]		Phenotype (J1/J2/Ig κ)[c]	*Fos/Jdp2/Batf* expression status[d]		
		PCR	Southern blotting		*Fos*	*Jdp2*	*Batf*
s1	T	+	G	2/1/G	−	1.5	−
s2	T	+	G	1/2, (1)/G	−	1.35, 1.5, 3.0, 4.4, 7.5	−
s3	T	+	n.d.	2/G, 1/G	n.d.	n.d.	n.d.
s4	T	+	G	G/2/G	−	1.5	−
s5	T	+	G, R	0/2/G	−	1.5	−
s6	T	+	G, R	G/G, 1/G	−	−	−
s7	T	+	n.d.	G/G, 2/G	−	1.5[e]	−
s8	T	+	G	n.d./n.d./n.d.	−	1.5[e]	−
s9	T	+	G	n.d./n.d./n.d.	n.d.	n.d.	n.d.
s10	T	+	n.d.	1/G/G	n.d.	n.d.	n.d.
s11	T	+	G	(1)/(G), 2/G	−	1.5	−
s11	m-L	−	G	G, 3/(G), 2/G	−	−	−
s12	T	+	G	G, (1)/(G), 2/G	−	3.0	−
s13	S	+	G	G/G/G	−	−	−
s13	t-L	+	G	G/G, (1)/G	−	−	−
s13	m-L	+	G	G/G, (1)/G	−	−	−
s14	T	+	G	1/2/G	−	1.5	−
s14	S	−	G	G/G/G	−	−	−
s15	m-L	+	n.d.	n.d./n.d./G	n.d.	1.5	n.d.
s16	T	+	G	2/G, 1/G	−	1.35	−
s16	S	+	G	G, 2/(G), 1/G	−	1.5, 7.5	−
s17	S	+	G	G/G, (2)/G	−	−	+
s17	m-L	−	G	G/G, (2)/G	−	−	−
s18	T	+	n.d.	G, 1/G, 1/n.d.	−	−	−
s18	S	+	n.d.	G, 1/G, 1/n.d.	−	−	−
s18	m-L	+	n.d.	G, 1/G, 1/n.d.	−	−	−
s19	T	+	n.d.	n.d./n.d./n.d.	n.d.	n.d.	n.d.
s19	S	n.d.	n.d.	n.d./n.d./n.d.	n.d.	n.d.	n.d.
s19	m-L	n.d.	n.d.	n.d./n.d./n.d.	n.d.	n.d.	n.d.
s20	T	+	n.d.	n.d./n.d./n.d.	n.d.	−	−
s20	m-L	n.d.	n.d.	n.d./n.d./n.d.	n.d.	−	−

n.d., not determined.

[a] Grossly enlarged lymphoid organs as observed upon necropsy, which are included in the present analysis: T, thymus; S, spleen; m-L and t-L, mesenteric and thoracic lymph node, respectively.

[b] The specific proviruses in the *Fos/Jdp2/Batf* region as detectable (+) or not detectable (−) by PCR, or by Southern blotting employing integration site specific probes detecting either the germ line (G) or a rearranged band of expected size (R).

[c] Rearrangement patterns of the J1 and J2 TCR β gene segments and Ig κ are described by a clonal germ line band (G) and/or the number of clonal rearrangements (between 1 and 3); 0 indicates that neither germ line nor rearranged band was observed whereas numbers in parenthesis denote faint bands only visible upon long time exposure.

[d] Northern blot expression data of *Fos/Jdp2/Batf* locus genes with increased mRNA levels (+) or levels comparable to control samples (−) as determined visually. Shown are sizes (kb) of *Jdp2* species with increased mRNA levels as determined visually and by densitometry (the 1.5 kb species).

[e] mRNA levels were higher than some but not all controls from the SL3-3/SWR model hindering conclusive interpretation regarding *Jdp2* mRNA levels (see text).

were clonal for rearrangements in the TCR β chain locus, whereas the Ig κ chain locus consistently had the germ line configuration (Fig. 2). Thus, in agreement with the well-established disease-inducing properties of SL3-3 (Ethelberg et al., 1997b; Hallberg et al., 1991; Hays et al., 1989; Lenz et al., 1982), lymphomas displayed a clonal T cell lineage origin with a few distinguishable rearranged hybridization bands. The general hybridization patterns in SL3-3-induced tumors harboring integrations in the locus were indistinguishable from those of the same tumor panel without integrations in the locus.

Two Akv-derived proviruses, in mouse s13 and s17, were identified in the 5′ and 3′ end, respectively, of the region analyzed here. Unexpectedly, lymphomas from these mice had detectable rearrangements in their TCR β chain locus (Fig. 3), a rare observation in Akv wt-induced tumors (Lovmand et al., 1998; Sørensen et al., 2004). The two proviruses were more than 200 kb apart and did not appear to influence the expression of a common gene (see below). We also addressed the clonality of the specific integrations by Southern blot analysis. In only two out of 13 mice investigated could a provirus-mediated rearrangement be detected (Table 3). Finally, we tested the presence of the specific *Fos/Jdp2/Batf* proviral integrations in peripheral lymphatic tissue not subjected to retroviral tagging analysis (see Materials and methods). The specific integrations in *Fos/Jdp2/Batf* were detectable by PCR in peripheral tissue of three (s13, s16 and s18) out of six mice investigated

Fig. 2. Phenotype characterization of SL3-3 induced tumors by Southern blot analysis. SL3-3 Runx II (lanes 1–6) and SL3-3 Runx I (lanes 7–11) induced thymic tumors of NMRI-r mice. Tumors harboring integrations into the *Fos/Jdp2/Batf* locus are lanes 1 (mouse s1), 4 (s2), 7 (s4) and 9 (s5), whereas tumors in lanes 2, 3, 5, 6, 8, 10, 11 had no integration into the locus. The positions of the unrearranged germ line bands are indicated to the left with a bar. The blot is representative for the majority of tumors analyzed here as summarizes in Table 3.

Fig. 3. Rearrangements of the TCR β chain J2 segment in tumors harboring an Akv-derived provirus in the *Fos/Jdp2/Batf* locus. Akv PBS_Lys (lanes 1–8) and Akv 1–99 Runx/GR + Akv wt (9–15) induced tumors of NMRI-i mice. Tumors from the *Fos/Jdp2/Batf* positive mice s13 and s17 are in lanes 4 (spleen), 5 (thoracic lymph node), 6 (mesenteric lymph node), and 11 (spleen) and 12 (mesenteric lymph node), respectively. Grossly enlarged organs from the controls are spleen (lanes 1, 7, 9, 10, 13–15) and mesenteric lymph node (lanes 2, 3 and 8). The positions of germ line and rearranged bands are indicated with a bar and arrows, respectively. In certain panels subjected to J2 probe hybridization, we observe hybridization bands of uncertain biological relevance (denoted with a star ('*')), which may represent NMRI-i confined pseudogene segments.

(Table 3). This, together with the Southern blot analysis of proviral rearrangement, indicates insertion into this locus to be a relatively late event in the SL3-3 model.

Activation of Jdp2 by SL3-3 insertional mutagenesis

The *Jdp2* mRNA levels in tumor tissue harboring integration in the locus were assessed by Northern blot hybridizations. Since genes of the *Fos/Jdp2/Batf* locus may directly or indirectly respond to common aspects of MLV infection and lymphomagenesis, we compared mRNA levels of *Fos/Jdp2/Batf*-positive mice to several mice of the same injection round but without *Fos/Jdp2/Batf* locus-specific integration.

Jin et al. (2001) reported of numerous *Jdp2* transcript species ranging from below 1 kb to above 9 kb in various tissues, whereas only a few were identified by Wardell et al. (2002); the reason for this disagreement is not clear. Transcripts of approximately 1.5 kb are currently supported by public sequence databases (UCSC October 2003 assembly). To elucidate this, and to look for possible provirus mediated activation of individual transcript species, we generated a 599-bp CDS residing probe covering exon 3 and part of exon 4 of *Jdp2* (Fig. 4A). Using this probe, Northern blot hybridizations revealed at least five differently sized *Jdp2* mRNAs in MLV-induced tumor tissues (Figs. 4D and E and data not shown). These were supplemented with hybridization on a mRNA⁺ Multiple-Tissue-Northern blot (ClonTech) using the same probe, identifying 10 different mRNA species expressed in a tissue-dependent manner (Fig. 4B). Furthermore, in a series of mouse cell lines, we identified four transcript species (Fig. 4C) that by size
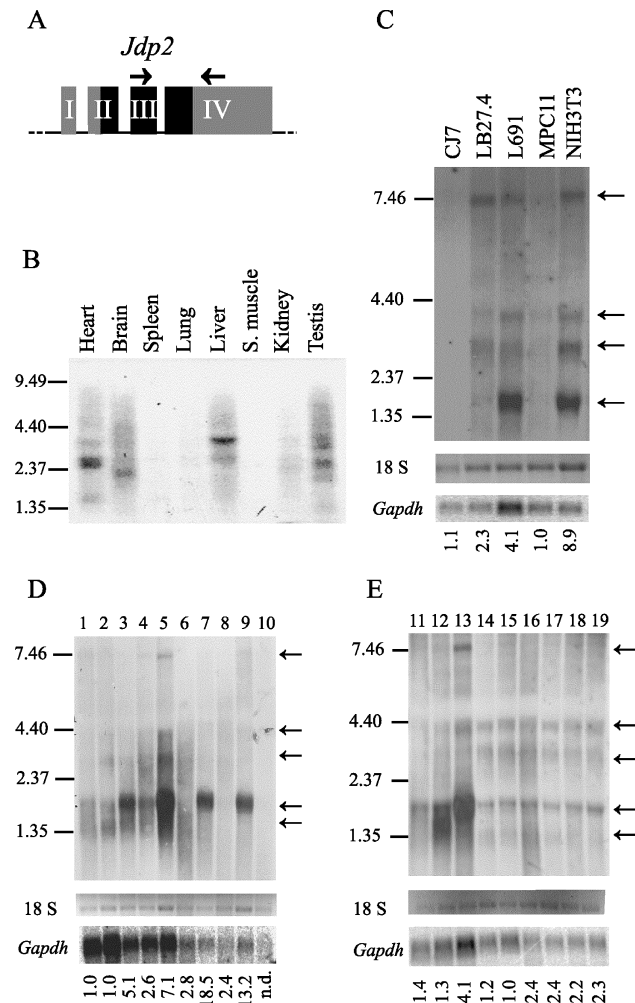
Fig. 4. Expression of *Jdp2* as assessed by Northern blot analysis. (A) Schematic illustration of the position in exons 3 and 4 of the primers used for generation of a 599-bp *Jdp2*-specific probe used throughout this study. CDS is shown in black. (B) and (C) Hybridization onto a MTN blot and cell line blot reveals an extensive tissue specific expression pattern of *Jdp2*. In (B), a 3-h exposure is shown. Upon longer exposure time, ~1.5 and ~3.0 kb bands emerge in the spleen, lung and kidney lanes, and very faintly in the skeleton muscle lane as well (not shown). Northern hybridization on RNA from tumors induced by SL3-3 Runx II (lanes 1–6) and SL3-3 Runx I (lanes 7–10) in NMRI-r mice (D), and Akv1-99 Egre /SL3-3 wt in NMRI-i (lanes 11–19) (E). Samples from mice with integration in the *Fos/Jdp2/Batf* locus are in lanes 3 (mouse s1), 5 (s2), 7 (s4), 9 (s5) and 12–13 (s16). The RNA was isolated from thymic (lanes 1–10 and 13) and splenic (lanes 11, 12 and 14–19) tumors. Position and size (in kb) of RNA marker bands are shown. Arrows indicate different transcript species. The 18 S ribosomal band was used as loading control, and *Gapdh* for even transfer of RNA onto membrane. The *Gapdh*-normalized hybridization signal of the 1.5-kb species is given below. Insufficient *Gapdh* hybridization signal in lane 10 impeded densitometrical analysis (n.d.).

corresponded to those seen in virus-induced tumor tissue. In addition to NIH3T3 fibroblasts, we note a higher expression in L691 T cells as compared to the B cell-related LB27.4 and MPC11, and the complete absence in embryonal CJ7. These results strongly support the notion of extensive alternative splicing of *Jdp2*.

Sixteen of the twenty mice with integration in the *Fos/Jdp2/Batf* locus were investigated with Northern blot analysis as summarized in Table 3. Of these, nine had increased levels of mainly the 1.5-kb *Jdp2* mRNA (Figs. 4D and E). In some tumors, however, other mRNA species (1.35 kb, 3.0 kb, 4,4 kb and 7.5 kb) were in abundance as compared to controls, although it should be emphasized that since these species were faintly expressed in control samples, this interpretation was based on visual inspection and not densitometrical data. One particular interesting case was seen in mouse s16 harboring an intronic integration between *Jdp2* exon 2 and exon 3. Whereas the thymic tumor of this mouse had elevated levels of the primary 1.5 kb as well as of a 8.0 kb transcript, the splenic tumor (that also contained the *Jdp2* specific provirus as found by PCR) showed elevation of a shorter 1.35 kb species (Fig. 4E). This positive correlation between provirus insertion and elevated levels of an alternative mRNA species suggests expression from a common transcriptional unit and hence adds further support for alternative splicing of *Jdp2*.

With the exception of the provirus in s16, all *Jdp2* activating integrations were positioned between *Jdp2* and *Fos*. The effect of the *Jdp2* intragenic integrations in s10 and s3, however, could not be investigated due to lack of primary material. The five *Jdp2-Batf* intergenic integrations (in s6, s18, s20, s8 and s17) appeared not to increase *Jdp2* mRNA levels in end-stage lymphomas (not shown). However, we found profound heterogeneity in *Jdp2* expression in the SL3-3 UCR/SWR model (not shown) that contrasted what was observed in the other models, and, since the SL3-3 UCR variant in SWR induces T lymphomas significantly faster (Ma et al., 2003), may be a result of heterogeneity within the tumor mass. Consequently, assessment of the *Jdp2* expression levels for s6, s7 and s8 was difficult, albeit in s6 *Jdp2* expression was lacking altogether and was hence considered negative for increased expression. Finally, the rather remote provirus in s13 (144 kb from *Jdp2*) also did not influence *Jdp2* expression.

Identification of Batf as a novel target of insertional mutagenesis

In addition to *Jdp2*, *Fos* and *Batf* could be additional targets for provirus insertions. From three different models, a total of four integrations have been found within 30 kb 5′ of *Fos* (Kim et al., 2003; Lund et al., 2002; Suzuki et al., 2002) and a single integration near *Batf* (Suzuki et al., 2002), yet the significance of these integrations in terms of altered transcription levels has not been investigated.

To clarify the expression level of the two genes, the Northern blot filters used for *Jdp2* hybridizations were stripped and reprobed with a *Fos* probe and finally a *Batf* probe. In none of the animals was *Fos* mRNA levels elevated (Table 3) suggesting that this gene was not targeted by the integrations. This was somewhat unexpected with regard to the integration in mouse s13 since this was

positioned in opposite transcriptional orientations within 30 kb of *Fos* similar to three of four previously published *Fos* integrations (Kim et al., 2003; Lund et al., 2002; Suzuki et al., 2002).

In mouse s17, one provirus was found integrated in the positive transcriptional orientation approximately 1.5 kb in front of *Batf*. Northern blotting hybridization was done with a probe covering the whole coding region of *Batf*. In all mice analyzed with integration into *Fos/Jdp2/Batf*, *Batf* mRNA levels equaled that of the controls, except the splenic tumor of s17, which gave a strong signal of the expected size (approximately 1 kb) (Fig. 5). A high intensity signal from the gene for glyceraldehyde-3-phosphate dehydrogenase (*Gapdh*) used for normalization nevertheless reduced the degree of *Batf* mRNA abundance. However, even ribosomal intensity signals across the EtBr-stained Northern gel strongly indicated the high *Gapdh* mRNA levels to be intrinsic to the splenic tumor of s17 as have previously been recognized in cancers of human and murine origin (Bhatia et al., 1994; Bustin, 2000; Finnegan et al., 1993).

To further clarify on this, SYBR Green real-time PCR relative quantification was performed to determine *Batf* mRNA levels in s17 as compared to controls. Normalization was done according to total RNA measured prior to cDNA synthesis (Bustin, 2000). The results agreed with the figure obtained by normalization with the 18 S signal intensity (Fig. 5) and suggested that *Batf* indeed was targeted by the Akv provirus inserted ~1.5 kb 5′ to the transcription start site. This, to our knowledge, is the first report of proviral activation of *Batf*.

The position and positive orientation of the provirus in s17 could allow for promoter activation of *Batf*. However, a changed transcript size indicative of such putative chimeric transcript was not seen on the Northern blot. This was supported by our inability to detect a virus-*Batf* transcript by directed reverse transcriptase PCR with primers specific to *Batf* and to the viral R or U5 regions (not shown).

Discussion

Virus distinct integration clustering in the Fos/Jdp2/Batf locus

In a comparative study involving 1190 mice inoculated with the B lymphomagenic Akv and the T lymphomagenic SL3-3 MLV, we have addressed the significance of proviral integrations into a locus that harbors the three AP-1/ATF super family genes *Fos*, *Jdp2* and *Batf* identified by high-throughput retroviral tagging. Hwang et al. have previously reported an increased frequency of integration into this region in M-MLV induced T lymphomas of p27-null C57/B6J × 129/Sv mice (Hwang et al., 2002).

The integration pattern in and around *Jdp2* by SL3-3 shows similarities but also distinguishable differences from those observed by the M-MLV study (Hwang et al., 2002). First, in that study, the number (as assessed by retroviral tagging and Southern blotting for *Jdp2* rearrangement) of mice with insertion in the *Fos-Jdp2* intergenic region and within *Jdp2* was three and six respectively, whereas in the SL3-3 MLV setting, ten mice had *Fos-Jdp2* insertions versus three with intragenic insertions. Notably, two M-MLV insertions are positioned in the major SL3-3 cluster 57 kb upstream of *Jdp2*. Second, only one of the intragenic insertions reported had a positive transcriptional orientation with respect to *Jdp2*, whereas all six intragenic proviruses identified in the M-MLV study had a positive transcriptional orientation, of which two enabled Jdp2 truncation by insertion between exons 2 and 3. Lack of primary material has prevented us from looking for virus−*Jdp2* fusion transcripts in the single mouse (s3) of this panel with a *Jdp2* intragenic integration comparable to those of the M-MLV study. Finally, we found a cluster of integrations between *Jdp2* and *Batf* that thus far is unique to the SL3-3 model.

The predominance of distinct *Fos/Jdp2/Batf* integrations in T cell lymphomas has recently been strengthened with the finding of two out of 41 MoFe2-MoLV inoculated NIH/Swiss mice with integration into the locus: one into *Jdp2*
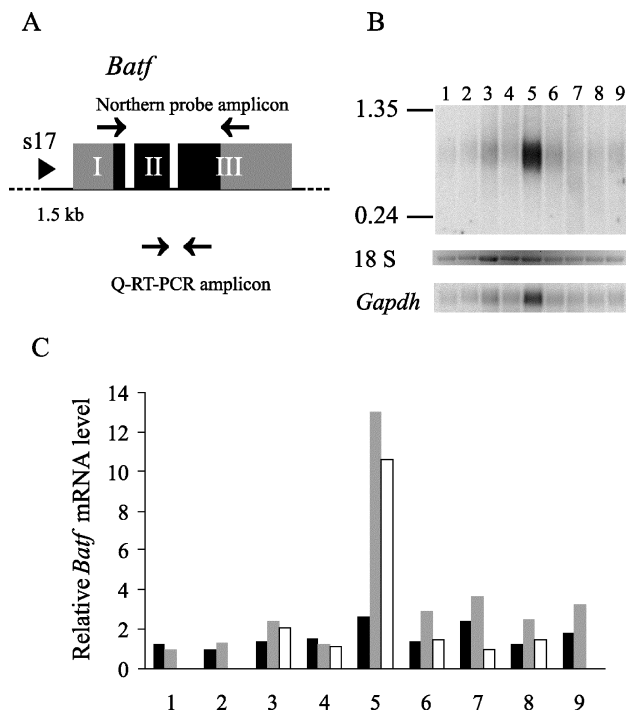

Fig. 5. Expression of *Batf*. (A) Schematic illustration of the primer positions used for generation the Northern blot probe (exons 1 and 3) and for quantification by real-time PCR (exons 2 and 3). The Akv-derived provirus in s17 positioned 1.5 kb 5′ of *Batf* exon 1 is indicated with a triangle. CDS indicated in black. (B) Northern blot hybridization with RNA from splenic (lanes 1–5 and 7–9) and mesenteric lymph node (lane 6) tumors from the Akv1–99 Runx + GR/Akv wt panel. RNA from s17 in lanes 5 and 6. (C) Relative expression of *Batf* as estimated by normalization to the *Gapdh* hybridization signal (black bars) or the intensity of the 18 S ribosomal band (gray bars), or when quantified with real-time PCR (white bars). Samples number as in (B).

intron 2 and the other in the major cluster between *Fos* and *Jdp2* (Johnson et al., 2005). Only two non-T cell lymphomas are listed in RTCGD as having integration into the locus, in both cases with positively oriented *Jdp2* intron 2 insertion: one M-MLV induced B cell lymphoma (among 27 inoculated EμMyc mice (Mikkers et al., 2002)) and one Cas-Br-M MLV induced myeloid leukemia (among 28 inoculated NFS/N mice (Joosten et al., 2002)). By comparing a similar number of Akv- and SL3-3-induced tumors, the lack of Akv activation in the *Fos/Jdp2/Batf* locus most clearly demonstrate this.

Larger cohorts will be needed to settle whether differences in mouse strain explain the absence of *Jdp2* integrations among 48 SL3-3 induced T lymphomas in NFS/N mice by Kim et al. (2003).

Insertional activation of multiple Jdp2 transcripts in SL3-3 induced T lymphomas

We assessed *Jdp2* mRNA levels in sixteen out of twenty animals with integration in the locus. Nine integrations correlated with elevated *Jdp2* mRNA levels of which eight were positioned between *Fos* and *Jdp2* while one was integrated between *Jdp2* exons 2 and 3. Notably, since the integrations into these tumors were sub-clonal, the degree of *Jdp2* overexpression may be vastly underestimated.

Jdp2 is expressed ubiquitously but some controversy seems to exist regarding the extent of alternative splicing (Jin et al., 2001; Wardell et al., 2002). Multiple transcripts could stem from promoter heterogeneity as suggested by database records (UCSC October 2003 assembly; http://www.genome.cse.ucsc.edu/index.html), however, alternative promoter usage seems inadequate to explain the larger (>3 kb) species observed. Thus, these must result from alternative splicing to hitherto unknown expressed sequences. In various cell lines and in normal tissue, including organs of the hematopoietic compartment, alternative splicing of *Jdp2* was prominent as assessed by Northern blotting. In virus induced tumor tissue, in addition to a major 1.5 kb transcript, which by size corresponds to the published species, multiple sub-transcripts were evident, and in some tumors harboring integration into *Fos/Jdp2/Batf* co-elevation of such sub-transcripts were seen. This adds substantial support to the notion that *Jdp2* indeed is alternatively spliced. Interestingly, in a number of *Fos/Jdp2/Batf*-positive tumors, elevation of *Jdp2* sub-species was predominant. The *Jdp2* intragenic provirus of s16 induced transcription of a smaller 1.35 kb form in the splenic but not thymic tumor. We have not revealed the nature of this transcript but speculate the provirus might activate transcription of exon three and four by enhancer activation of an internal promoter residing in *Jdp2* intron 2. RNA from the other mouse (s10) with a provirus inserted similar as in s16 was not attainable for Northern blot analysis and therefore the significance of the observation could not be evaluated further. It is possible that the mechanism of *Jdp2* activation

in s16 and s10 mimics that of the above-mentioned models with positively oriented intron 2 proviruses (Hwang et al., 2002; Johnson et al., 2005; Joosten et al., 2002; Mikkers et al., 2002), however, the identities of the activated *Jdp2* transcripts was not revealed (Hwang et al., 2002), or *Jdp2* expression analysis not done (Johnson et al., 2005; Joosten et al., 2002; Mikkers et al., 2002).

Batf is a target of insertional activation

This study identifies *Batf* as a novel target of insertional mutagenesis. Only a single integration correlated with increased *Batf* mRNA levels and it is therefore not possible to evaluate its significance to tumorigenesis. Interestingly, without clarifying on the expression level of *Batf*, Suzuki et al. have also found a single SL3-3 derived provirus 1.8 kb upstream of *Batf*, albeit in the opposite transcriptional orientation (Suzuki et al., 2002). *Batf* expression appears restricted to the hematopoietic compartment (Echlin et al., 2000; Williams et al., 2001, 2003) and has been correlated with HTLV-1- and EBV-infected cells (Dorsey et al., 1995; Hasegawa et al., 1996; Johansen et al., 2003). Furthermore, since its co-expression blocks Fos- and Ras-dependent transformation by negatively regulating AP-1 activity (Echlin et al., 2000; Williams et al., 2001), it would be interesting to determine under which circumstances its activation by insertional mutagenesis is selected for during lymphomagenesis.

In mouse s13, the integration upstream of *Fos* did not alter the expression of *Fos* as assessed by Northern blotting. Since this integration was sub-clonal, we cannot rule out the possibility that an impact on *Fos* expression has been shielded by other clonal lineages of the tumor mass. It would thus be important to know the clonality as well as the expression status of four previously reported cases of *Fos* insertion (Kim et al., 2003; Lund et al., 2002; Suzuki et al., 2002) to learn if this position represents a 'silent' common integration site that may inform of subtle selection effects during lymphomagenesis, as discussed below.

The Jdp2-Batf intergenic CIS is unique to SL3-3 MLV tumorigenesis

Six integrations (in s10, s6, s18, s8, s20 and s9) were identified in opposite transcriptional orientation between CDS of *Jdp2* and *Batf* and define a common integration site not reported elsewhere. Normal levels of *Jdp2* and *Batf* were present in s6, s18 and s20. *Batf* mRNA level in s8 was normal, while expression heterogeneity in the SL3-3 UCR/SWR model, as discussed above, impeded conclusive interpretations regarding *Jdp2* for this tumor. Mouse s10 and s9 were not assessed but given their position and orientation common to s6 and s18, s8 and s20, respectively, it seems conceivable that these integrations also are neutral with respect to mRNA levels of the neighboring genes *Jdp2* and *Batf*. Bearing in mind the sub-clonality of the tumors,

integration by SL3-3 MLV within *Jdp2* and *Batf* may thus be neutral in end-stage tumors. It is possible that apparently 'neutral' integration sites, without evidence of altered transcription, affect genes outside the region considered through long-range interactions (Lazo et al., 1990). However, less recognized mechanisms might influence the selection of common integration sites among fully developed tumors such as perturbation of transcription control through interruption of chromatin structure (Bode et al., 2003), or triggering of host RNA interference pathways as observed for inherited retroelements of eukaryotes (Shi et al., 2004; Svoboda et al., 2004). Moreover, very little is currently known about the transcription status of virally activated host genes throughout tumor development. Are some host genes virally activated during early stages, and then later, pre-neoplastic cells progress through selection for reduced activation of the same genes (Hanlon et al., 2003)?

Does model distinct integration patterns reflect distinct tumor etiologies?

The type of lymphoma/leukemia generated in susceptible mice by murine leukemia viruses is a function of both virus and mouse strain utilized. Activation by insertional mutagenesis of certain oncoloci in current models correlate with major tumor phenotypes of the T cell (e.g., *Rras2*), B cell (*Sox4/Evi16*) and myeloid (*Evi1*) lineages (see RTGCD), to some degree resembling the diagnostic value of distinct translocations in human leukemia (Vega and Medeiros, 2003). Conversely, distinct integration patterns among related models may be indicative of different tumor etiology. For instance, the SL3-3 Turbo enhancer variant, which displays a significant shortened lymphoma latency in NMRI mice (Ethelberg et al., 1997c), has distinct integration hotspots in the c-*myc* promoter region as compared to SL3-3 wt (Nielsen et al., 2005). Similarly, the distinct integration pattern into the *Fos/Jdp2/Batf* locus in SL3-3 and M-MLV induced T cell lymphomagenesis indicate that *Jdp2* contributes differently to lymphomagenesis in the two models. Such notion may find support in the observation that integrations into the locus generally are sub-clonal in the SL3-3 setting but clonal in the M-MLV model.

An obvious consideration is the influence on tumorigenesis by the host genetic background. We note a high representation of *Fos/Jdp2/Batf* locus insertions between SL3-3-induced lymphomas from random-bred NMRI (5/58) as compared to inbred NMRI mice (6/327), irrespective of the virus sub-variant.

On a defined background (C57/BJ6 x 129/Sv), Hwang et al. (2002) observed an increased frequency of provirally mediated *Jdp2* rearrangements in p27-null as compared to wt mice (two versus seven among 25 tumor samples). Considering this, it cannot be formally ruled out that increased insertion frequency in the SWR and random-bred NMRI strains reported here results from a heritable genetic

impairment of the p27^{Kip1} pathway and not from differences in virus utilization. Although SL3-3 and M-MLV hold binding sites motifs in common (Golemis et al., 1990), variations between the viral enhancers indicate adaptation to distinct cell types, which consequently could imply different routes of T lymphoma induction. Dissimilar enhancer activities in lymphoid and non-lymphoid cells in vitro supports such notion (Couture et al., 1994; LoSardo et al., 1989; Short et al., 1987). Importantly, a binding site motif for c-Myb is absent from the M-MLV enhancer, yet its presence in SL3-3 is of critical importance to the lymphomagenesis of this virus (Nieves et al., 1997). Similarly, the single most important binding site motif of the M-MLV, the LVb site (Speck et al., 1990), appears of negligible importance to SL3-3 pathogenicity (Nieves et al., 1997).

In summary, among twenty individual MLV induced lymphomas in a screen counting 1190 sample species, we have identified twenty-two T cell lymphoma specific integrations in the *Fos/Jdp2/Batf* locus, previously reported to be targeted in an M-MLV setting (Hwang et al., 2002). *Jdp2* and, in a single case, *Batf* mRNA levels correlated positively with provirus insertions, however, a rather large fraction of the proviruses integrated into a novel common integration site that apparently remained silent with respect to transcriptional status of the investigated genes. Distinct integration patterns among models must reflect separate selection paths during tumor development, and as such, hold information regarding retroviral insertion mutagenesis mechanisms in vivo and the nature of activation of individual proto-oncogenes in viral and non-viral models.

Materials and methods

Tumor panels and isolation of retroviral tags

Archival frozen tumors samples originated from published and unpublished pathogenicity studies on Akv, SL3-3 and derivatives hereof (see Tables 1 and 2). From each animal, tumor DNA from one organ (thymus if injected with SL3-3, and spleen or lymph node if injected with Akv or Akv + SL3-3) was analyzed.

These tumor DNAs were studied as part of a large scale retroviral tagging screen performed at Sagres Discovery (Davis, CA) (Morris, 2003). Using a process called High-Throughput Provirus Tagging (HPT), approximately 16,000 tags from 5500 tumors had been isolated and mapped to the mouse genome at the time the dataset for this report was assembled. Host/virus junction fragments from integrated proviruses were amplified by anchored-PCR, gel purified, cloned and sequenced, using standard techniques. The host flanking sequences were then mapped onto the UCSC October 2003 mouse genome assembly to determine the provirus integration patterns at loci activated by insertional mutagenesis.

Cell cultures

MPC11 murine myeloma/plasmacytoma B cells and NIH 3T3 murine fibroblasts were grown in Dulbecco's modified Eagle's medium containing Glutamax-1 (Gibco) supplemented with 10% Fetal Bovine Serum or Newborn Calf Serum (NCS), respectively. T lymphoma-derived L691 cells (McGrath et al., 1980) were grown in RPMI medium with Glutamax-1 and supplemented 10% NCS. To all media were added 100 U of penicillin and 100 μg of streptomycin per ml. Murine CJ7 ES cells (Swiatek and Gridley, 1993) were grown as described (Hansen et al., 2003). The B cell hybridoma LB27.4 cell line was grown as described previously (Tolstrup et al., 2001).

Total RNA was extracted using TRIzol (Invitrogen) according to manufacturer's recommendations.

Northern and Southern blot hybridizations

Genomic DNA was extracted from frozen tumor tissue with the DNeasy Tissue Kit (Qiagen). From each sample, 20 μg was digested to completion with HindIII, resolved on a 1.2% agarose gel, transferred to a Zeta-Probe membrane (Bio-Rad) in 0.4 M NaOH by capillary force and subjected to Southern blot hybridization as described previously (Ethelberg et al., 1997a). For Northern blotting, 20 μg of TRIzol (Invitrogen)-extracted total RNA per tumor sample was denatured in formamide and 37% formaldehyde at 65 °C and then electrophoresed in a 1.2% denaturing formaldehyde gel in MOPS buffer. RNA was transferred to a Zeta-Probe (Bio-Rad) membrane in 50 mM NaOH and finally subjected to hybridization as described (Sørensen et al., 2000). To estimate mRNA levels of *Fos*, *Jdp2* and *Batf*, the membrane was exposed to a phosphoimager screen, developed in a Molecular Imager FX and expression signal evaluated relative to *Gapdh* mRNA levels using PhosphoImager software (Bio-Rad). Expression levels in individual tumors with integration into *Fos/Jdp2/Batf* were compared on the same blot against 6–8 tumors from the same injection round but without integration into the locus (control samples). Hybridization with the mRNA^{+} Multiple-Tissue-Northern (ClonTech) was done according to the manufacturer's recommendations. DNA and RNA were quantified by spectrophotometric means and their integrity confirmed by gel electrophoresis.

Quantitative real-time PCR

Real-time PCR was done on a Stratagene MX4000 using Brilliant SYBR 1 chemistry (Stratagene). For each reaction, cDNA (First-Strand cDNA Kit (Amersham Biosciences)) originating from 30 ng of total RNA as measured by a Genequant II spectrophotometer was used. Initial *Batf* mRNA copy numbers were evaluated using a standard curve from an unrelated MLV-induced splenic tumor run simultaneously. All reactions were carried out in triplicates.

References

Akagi, K., Suzuki, T., Stephens, R.M., Jenkins, N.A., Copeland, N.G., 2004. RTCGD: retroviral tagged cancer gene database. Nucleic Acids Res. 32 (90001), D523–D527.

Aronheim, A., Zandi, E., Hennemann, H., Elledge, S.J., Karin, M., 1997. Isolation of an AP-1 repressor by a novel method for detecting protein–protein interactions. Mol. Cell. Biol. 17 (6), 3094–3102.

Bhatia, P., Taylor, W.R., Greenberg, A.H., Wright, J.A., 1994. Comparison of glyceraldehyde-3-phosphate dehydrogenase and 28S-ribosomal RNA gene expression as RNA loading controls for Northern blot analysis of cell lines of varying malignant potential. Anal. Biochem. 216 (1), 223–226.

Blazek, E., Wasmer, S., Kruse, U., Aronheim, A., Aoki, M., Vogt, P.K., 2003. Partial oncogenic transformation of chicken embryo fibroblasts by Jun dimerization protein 2, a negative regulator of TRE- and CRE-dependent transcription. Oncogene 22 (14), 2151–2159.

Bode, J., Goetze, S., Heng, H., Krawetz, S.A., Benham, C., 2003. From DNA structure to gene expression: mediators of nuclear compartmentalization and dynamics. Chromosome Res. 11 (5), 435–445.

Broder, Y.C., Katz, S., Aronheim, A., 1998. The ras recruitment system, a novel approach to the study of protein–protein interactions. Curr. Biol. 8 (20), 1121–1124.

Bustin, S.A., 2000. Absolute quantification of mRNA using real-time reverse transcription polymerase chain reaction assays. J. Mol. Endocrinol. 25 (2), 169–193.

Couture, L.A., Mullen, C.A., Morgan, R.A., 1994. Retroviral vectors containing chimeric promoter/enhancer elements exhibit cell-type-specific gene expression. Hum. Gene Ther. 5 (6), 667–677.

Dorsey, M.J., Tae, H.J., Sollenberger, K.G., Mascarenhas, N.T., Johansen, L.M., Taparowsky, E.J., 1995. B-ATF: a novel human bZIP protein that associates with members of the AP-1 transcription factor family. Oncogene 11 (11), 2255–22565.

Echlin, D.R., Tae, H.J., Mitin, N., Taparowsky, E.J., 2000. B-ATF functions as a negative regulator of AP-1 mediated transcription and blocks cellular transformation by Ras and Fos. Oncogene 19 (14), 1752–1763.

Erkeland, S.J., Valkhof, M., Heijmans-Antonissen, C., Van Hoven-Beijen, A., Delwel, R., Hermans, M.H., Touw, I.P., 2004. Large-scale identification of disease genes involved in acute myeloid leukemia. J. Virol. 78 (4), 1971–1980.

Ethelberg, S., Hallberg, B., Lovmand, J., Schmidt, J., Luz, A., Grundström, T., Pedersen, F.S., 1997a. Second-site proviral enhancer alterations in lymphomas induced by enhancer mutants of SL3-3 murine leukemia virus: negative effect of nuclear factor 1 binding site. J. Virol. 71 (2), 1196–1206.

Ethelberg, S., Lovmand, J., Schmidt, J., Luz, A., Pedersen, F.S., 1997b. Increased lymphomagenicity and restored disease specificity of AML1 site (core) mutant SL3-3 murine leukemia virus by a second-site enhancer variant evolved in vivo. J. Virol. 71 (10), 7273–7280.

Ethelberg, S., Sørensen, A.B., Schmidt, J., Luz, A., Pedersen, F.S., 1997c. An SL3-3 murine leukemia virus enhancer variant more pathogenic than the wild type obtained by assisted molecular evolution in vivo. J. Virol. 71 (12), 9796–9799.

Finnegan, M.C., Goepel, J.R., Hancock, B.W., Goyns, M.H., 1993. Investigation of the expression of housekeeping genes in non-Hodgkin's lymphoma. Leuk. Lymphoma 10 (4–5), 387–393.

Golemis, E.A., Speck, N.A., Hopkins, N., 1990. Alignment of U3 region sequences of mammalian type C viruses: identification of highly conserved motifs and implications for enhancer design. J. Virol. 64 (2), 534–542.

Hallberg, B., Schmidt, J., Luz, A., Pedersen, F.S., Grundström, T., 1991. SL3-3 enhancer factor 1 transcriptional activators are required for tumor formation by SL3-3 murine leukemia virus. J. Virol. 65 (8), 4177–4181.

Hanlon, L., Barr, N.I., Blyth, K., Stewart, M., Haviernik, P., Wolff, L., Weston, K., Cameron, E.R., Neil, J.C., 2003. Long-range effects of retroviral insertion on c-myb: overexpression may be obscured by silencing during tumor growth in vitro. J. Virol. 77 (2), 1059–1068.

Hansen, G.M., Skapura, D., Justice, M.J., 2000. Genetic profile of insertion mutations in mouse leukemias and lymphomas. Genome Res. 10 (2), 237–243.

Hansen, J., Floss, T., Van Sloun, P., Fuchtbauer, E.-M., Vauti, F., Arnold, H.-H., Schnutgen, F., Wurst, W., von Melchner, H., Ruiz, P., 2003. A large-scale, gene-driven mutagenesis approach for the functional analysis of the mouse genome. Proc. Natl. Acad. Sci. 100 (17), 9918–9922.

Hasegawa, H., Utsunomiya, Y., Kishimoto, K., Tange, Y., Yasukawa, M., Fujita, S., 1996. SFA-2, a novel bZIP transcription factor induced by human T-cell leukemia virus type I, is highly expressed in mature lymphocytes. Biochem. Biophys. Res. Commun. 222 (1), 164–170.

Hays, E.F., Bristol, G.C., McDougall, S., Klotz, J.L., Kronenberg, M., 1989. Development of lymphoma in the thymus of AKR mice treated with the lymphomagenic virus SL 3-3. Cancer Res. 49 (15), 4225–4230.

Heinrich, R., Livne, E., Ben-Izhak, O., Aronheim, A., 2004. The c-Jun dimerization protein 2 inhibits cell transformation and acts as a tumor suppressor gene. J. Biol. Chem. 279 (7), 5708–5715.

Hwang, H.C., Martins, C.P., Bronkhorst, Y., Randel, E., Berns, A., Fero, M., Clurman, B.E., 2002. Identification of oncogenes collaborating with p27Kip1 loss by insertional mutagenesis and high-throughput insertion site analysis. Proc. Natl. Acad. Sci. U.S.A. 99 (17), 11293–11298.

Jin, C., Ugai, H., Song, J., Murata, T., Nili, F., Sun, K., Horikoshi, M., Yokoyama, K.K., 2001. Identification of mouse Jun dimerization protein 2 as a novel repressor of ATF-2. FEBS Lett. 489 (1), 34–41.

Jin, C., Li, H., Murata, T., Sun, K., Horikoshi, M., Chiu, R., Yokoyama, K.K., 2002. JDP2, a repressor of AP-1, recruits a histone deacetylase 3 complex to inhibit the retinoic acid-induced differentiation of F9 cells. Mol. Cell. Biol. 22 (13), 4815–4826.

Johansen, L.M., Deppmann, C.D., Erickson, K.D., Coffin III, W.F., Thornton, T.M., Humphrey, S.E., Martin, J.M., Taparowsky, E.J., 2003. EBNA2 and activated Notch induce expression of BATF. J. Virol. 77 (10), 6029–6040.

Johnson, C., Lobelle-Rich, P.A., Puetter, A., Levy, L.S., 2005. Substitution of feline leukemia virus long terminal repeat sequences into murine leukemia virus alters the pattern of insertional activation and identifies new common insertion sites. J. Virol. 79 (1), 57–66.

Joosten, M., Vankan-Berkhoudt, Y., Tas, M., Lunghi, M., Jenniskens, Y., Parganas, E., Valk, P.J., Lowenberg, B., van den Akker, E., Delwel, R., 2002. Large-scale identification of novel potential disease loci in mouse leukemia applying an improved strategy for cloning common virus integration sites. Oncogene 21 (47), 7247–7255.

Kawaida, R., Ohtsuka, T., Okutsu, J., Takahashi, T., Kadono, Y., Oda, H., Hikita, A., Nakamura, K., Tanaka, S., Furukawa, H., 2003. Jun dimerization protein 2 (JDP2), a member of the AP-1 family of transcription factor, mediates osteoclast differentiation induced by RANKL. J. Exp. Med. 197 (8), 1029–1035.

Kim, R., Trubetskoy, A., Suzuki, T., Jenkins, N.A., Copeland, N.G., Lenz, J., 2003. Genome-based identification of cancer genes by proviral tagging in mouse retrovirus-induced T-cell lymphomas. J. Virol. 77 (3), 2056–2062.

Lazo, P.A., Lee, J.S., Tsichlis, P.N., 1990. Long-distance activation of the Myc protooncogene by provirus insertion in Mlvi-1 or Mlvi-4 in rat T-cell lymphomas. Proc. Natl. Acad. Sci. U.S.A. 87 (1), 170–173.

Lenz, J., Crowther, R., Klimenko, S., Haseltine, W., 1982. Molecular cloning of a highly leukemogenic, ecotropic retrovirus from an AKR mouse. J. Virol. 43 (3), 943–951.

Li, J., Shen, H., Himmel, K.L., Dupuy, A.J., Largaespada, D.A., Nakamura, T., Shaughnessy Jr., J.D., Jenkins, N.A., Copeland, N.G., 1999. Leukaemia disease genes: large-scale cloning and pathway predictions. Nat. Genet. 23 (3), 348–353.

LoSardo, J.E., Cupelli, L.A., Short, M.K., Berman, J.W., Lenz, J., 1989. Differences in activities of murine retroviral long terminal repeats in cytotoxic T lymphocytes and T-lymphoma cells. J. Virol. 63 (3), 1087–1094.

Lovmand, J., Sørensen, A.B., Schmidt, J., Østergaard, M., Luz, A., Pedersen, F.S., 1998. B-Cell lymphoma induction by akv murine leukemia viruses harboring one or both copies of the tandem repeat in the U3 enhancer. J. Virol. 72 (7), 5745–5756.

Lund, A.H., Schmidt, J., Luz, A., Sørensen, A.B., Duch, M., Pedersen, F.S., 1999. Replication and pathogenicity of primer binding site mutants of SL3-3 murine leukemia viruses. J. Virol. 73 (7), 6117–6122.

Lund, A.H., Turner, G., Trubetskoy, A., Verhoeven, E., Wientjens, E., Hulsman, D., Russell, R., DePinho, R.A., Lenz, J., van Lohuizen, M., 2002. Genome-wide retroviral insertional tagging of genes involved in cancer in Cdkn2a-deficient mice. Nat. Genet. 32 (1), 160–165.

Ma, S.L., Lovmand, J., Sørensen, A.B., Luz, A., Schmidt, J., Pedersen, F.S., 2003. Triple basepair changes within and adjacent to the conserved YY1 motif upstream of the U3 enhancer repeats of SL3-3 murine leukemia virus cause a small but significant shortening of latency of T-lymphoma induction. Virology 313 (2), 638–644.

McGrath, M.S., Pillemer, E., Kooistra, D., Wissman, I.L., 1980. Contemporary Topics in Immunobiology. Plenum Publishing Corp., New York.

Mikkers, H., Allen, J., Knipscheer, P., Romeijn, L., Hart, A., Vink, E., Berns, A., Romeyn, L., 2002. High-throughput retroviral tagging to identify components of specific signaling pathways in cancer. Nat. Genet. 32 (1), 153–159.

Morris, D.W., 2003. Identification and characterization of the oncogenome using a mouse-to-human strategy. Presented at the 94th Annual Meeting of the American Cancer Society, Washington, DC.

Nielsen, A.A., Sørensen, A.B., Schmidt, J., Pedersen, F.S., 2005. Analysis of wild-type and mutant SL3-3 murine leukemia virus insertions in the c-*myc* promoter during lymphomagenesis reveals target site hot spots, virus-dependent patterns, and frequent error-prone gap repair. J. Virol. 79 (1), 1–12.

Nieves, A., Levy, L.S., Lenz, J., 1997. Importance of a c-Myb binding site for lymphomagenesis by the retrovirus SL3-3. J. Virol. 71 (2), 1213–1219.

Ostrovsky, O., Bengal, E., Aronheim, A., 2002. Induction of terminal differentiation by the c-Jun dimerization protein JDP2 in C2 myoblasts and rhabdomyosarcoma cells. J. Biol. Chem. 277 (42), 40043–40054.

Piu, F., Aronheim, A., Katz, S., Karin, M., 2001. AP-1 repressor protein JDP-2: inhibition of UV-mediated apoptosis through p53 down-regulation. Mol. Cell. Biol. 21 (9), 3012–3024.

Rosenberg, N., Jolicoeur, P., 1997. Retroviral Pathogenesis. In: Coffin, J.M., Hughes, S.H., Varmus, H.E. (Eds.), Cold Spring Harbor Laboratory Press, pp. 475–585.

Shi, H., Djikeng, A., Tschudi, C., Ullu, E., 2004. Argonaute protein in the early divergent eukaryote *Trypanosoma brucei*: control of small interfering RNA accumulation and retroposon transcript abundance. Mol. Cell. Biol. 24 (1), 420–427.

Short, M.K., Okenquist, S.A., Lenz, J., 1987. Correlation of leukemogenic potential of murine retroviruses with transcriptional tissue preference of the viral long terminal repeats. J. Virol. 61 (4), 1067–1072.

Sørensen, A.B., Duch, M., Amtoft, H.W., Jørgensen, P., Pedersen, F.S., 1996. Sequence tags of provirus integration sites in DNAs of tumors induced by the murine retrovirus SL3-3. J. Virol. 70 (6), 4063–4070.

Sørensen, A.B., Lund, A.H., Ethelberg, S., Copeland, N.G., Jenkins, N.A.,

Pedersen, F.S., 2000. Sint1, a common integration site in SL3-3-induced T-cell lymphomas, harbors a putative proto-oncogene with homology to the septin gene family. J. Virol. 74 (5), 2161–2168.

Sørensen, K.D., Quintanilla-Martinez, L., Kunder, S., Schmidt, J., Pedersen, F.S., 2004. Mutation of all runx (AML1/Core) sites in the enhancer of T-lymphomagenic SL3-3 murine leukemia virus unmasks a significant potential for myeloid leukemia induction and favors enhancer evolution toward induction of other disease patterns. J. Virol. 78 (23), 13216–13231.

Speck, N.A., Renjifo, B., Golemis, E., Fredrickson, T.N., Hartley, J.W., Hopkins, N., 1990. Mutation of the core or adjacent LVb elements of the Moloney murine leukemia virus enhancer alters disease specificity. Genes Dev. 4 (2), 233–242.

Suzuki, T., Shen, H., Akagi, K., Morse, H.C., Malley, J.D., Naiman, D.Q., Jenkins, N.A., Copeland, N.G., 2002. New genes involved in cancer identified by retroviral tagging. Nat. Genet. 32 (1), 166–174.

Svoboda, P., Stein, P., Anger, M., Bernstein, E., Hannon, G.J., Schultz, R.M., 2004. RNAi and expression of retrotransposons MuERV-L and IAP in preimplantation mouse embryos. Dev. Biol. 269 (1), 276–285.

Swiatek, P.J., Gridley, T., 1993. Perinatal lethality and defects in hindbrain development in mice homozygous for a targeted mutation of the zinc finger gene Krox20. Genes Dev. 7 (11), 2071–2084.

Tolstrup, A.B., Duch, M., Dalum, I., Pedersen, F.S., Mouritsen, S., 2001. Functional screening of a retroviral peptide library for MHC class I presentation. Gene 263 (1–2), 77–84.

Vega, F., Medeiros, L.J., 2003. Chromosomal translocations involved in non-Hodgkin lymphomas. Arch. Pathol. Lab. Med. 127 (9), 1148–1160.

Wardell, S.E., Boonyaratanakornkit, V., Adelman, J.S., Aronheim, A., Edwards, D.P., 2002. Jun dimerization protein 2 functions as a progesterone receptor N-terminal domain coactivator. Mol. Cell. Biol. 22 (15), 5451–5466.

Williams, K.L., Nanda, I., Lyons, G.E., Kuo, C.T., Schmid, M., Leiden, J.M., Kaplan, M.H., Taparowsky, E.J., 2001. Characterization of murine BATF: a negative regulator of activator protein-1 activity in the thymus. Eur. J. Immunol. 31 (5), 1620–1627.

Williams, K.L., Zullo, A.J., Kaplan, M.H., Brutkiewicz, R.R., Deppmann, C.D., Vinson, C., Taparowsky, E.J., 2003. BATF transgenic mice reveal a role for activator protein-1 in NKT cell development. J. Immunol. 170 (5), 2417–2426.